18th International Conference on Information Fusion
Washington, DC - July 6-9, 2015

Multistatic tracking experiment with a WiFiRAD passive radar

Maciej Wielgo, Stanisław Rzewuski, Jacek Misiurewicz, Anna Kurowska, Mateusz Malanowski
Institute of Electronic Systems
Warsaw University of Technology
Warszawa, Poland
{m.wielgo, s.rzewuski}@stud.elka.pw.edu.pl, {jmisiure, a.kurowska, m.malanowski}@elka.pw.edu.pl

***Abstract*—Abstract - A Wi-Fi based passive radar can be used for localization of objects in the vicinity of several access points, which are used as illumination sources. However, the transmission of Wi-Fi signal is not continuous – the activity of access points depends on the transmitted data and is totally unpredictable from the passive radar point of view. As a result, the ability to detect and measure an object using a given transmitter illumination changes at random. Thus, it is not possible to use a traditional Kalman filter with update of full Cartesian measurement. Instead we propose to use a filter with sequential update, where the object state is updated with a single measurement of bistatic range whenever it is available.**

The paper presents results of an experiment with live data, where an object was localized with use of an experimental Wi-Fi based passive radar (WiFiRAD) constructed at Warsaw University of Technology.

***Index Terms*—Multistatic tracking, PCL, Passive radar, Wi-Fi, sequential Kalman filter**

I. Introduction

The principle of passive radar is to use existing radio transmitters as illumination sources and measure waves reflected from the target [1]. The reflected (echo) signal is received with a correlation receiver using a separate antenna to acquire a transmitted signal (via direct path) to be used as a template. As the result of correlation processing, the delay between template and echo signals is measured. Additionally, the Doppler shift between signals may be also estimated.

A delay measurement from a single transmitter-receiver pair locates the target ambiguously – on an ellipse (or an ellipsoid in 3D space). In practical installations an omnidirectional antenna is used for the reflected signal, so the angle of arrival is not measured. Thus, in order to uniquely localize the target more measurements are needed. Usually a number of non-collocated transmitter-receiver pairs is used, making the localization and tracking problem a multistatic one.

The properties of a passive radar system depend strongly on the choice of illumination signal [2]–[4]. It is obvious that the range resolution depends on the bandwidth of the signal, which makes it necessary in some GSM-based radars to exploit Doppler information for localization [5]. When Wi-Fi node transmission is used for illumination of the scene, the packet-based nature of the signal and multiple access features of the network become an important problem [6]. The transmission of each node depends on the traffic and the timing is the result of complex arbitration between co-users of the network. Thus, the availability of measurements from all the transmitters is not guaranteed.

On the other hand, the addresses contained in the packet preamble allow the receiver to recognize the source of the signal, thus enabling separation of the echoes originating from different transmitters.

Results published up to date by the authors [7], [8] as well as by other researchers [9] have demonstrated success in detecting a target in mono-, bi-, and multistatic configurations of a Wi-Fi based passive radar.

Other authors investigated a topology influence on the performance of a Wi-Fi based radar using mathematical analysis and simulations [10]. Also many experiments with location and tracking have been done [11], [12]. They however do not deal with the problem of unavailable detections, which is an important point in this paper.

This paper extends the previous work by introducing tracking of an object with live data from a multistatic experiment and by applying sequential update in tracking filter in order to solve the problem of random timing and nonuniform availability of measurements.

The data were obtained in August 2014 from an experiment, where five Wi-Fi nodes connected in a network served as illuminators. The passive radar receiver was constructed using a set of off-the-shelf antennas and a laboratory vector signal analyzer.

II. Passive radar basics

Nowadays passive radars gain a lot of popularity in military as well as in civil applications. To detect objects and track their localization, passive radars use the external radiation source like: GSM stations, Wi-Fi stations, radio stations. The positions of transmitter and receiver are different so the bistatic geometry must be used.

We will concentrate on a setup in which the positions of the transmitter and the receiver do not change, but the reflecting object is moving. The distances between a target object and transmitter $R_{to}(t)$ and between a target object and receiver $R_{or}(t)$ are then described by following equations:

$$\begin{aligned} R_{to}(t) &= \sqrt{(x_t - x(t))^2 + (y_t - y(t))^2 + (z_t - z(t))^2} \\ R_{or}(t) &= \sqrt{(x_r - x(t))^2 + (y_r - y(t))^2 + (z_r - z(t))^2} \end{aligned} \quad (1)$$

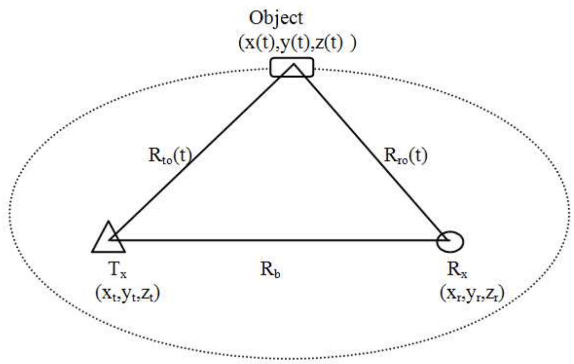

Fig. 1. Position of target object

A passive radar compares the measurement signal which travels the distance $R_{to}(t) + R_{or}(t)$, with the reference signal which travels the distance R_b between the transmitter and receiver. The measured delay between signals is thus proportional to $R(t)$ which is

$$R(t) = R_{to}(t) + R_{or}(t) - R_b \tag{2}$$

The solution to an inverse problem – i.e. finding a location of an object given the measured instantaneous value of $R(t)$ is an ellipse with foci at the transmitter and receiver locations (Fig. 1).

To determine the position of the object unambiguously we may use multiple external radiation sources (multistatic system). Then the location of the object is determined by the intersection of ellipses corresponding to each of the transmitter-receiver pairs.

The measurement of the delay (and in consequence the range $R(t)$ is performed by correlating the echo signal with the template constructed from the reference signal and its copies shifted in frequency – the result is a range-Doppler map of the echoes. In both range and Doppler dimension the map shows bistatic measurements.

As a rule, the longer is the correlation time, the higher is the gain in signal to noise ratio at the correlator output. Moreover, with long correlation times the Doppler frequency resolution increases. In a packet radio (e.g. Wi-Fi) based radar the gaps in the transmission from a single source make it, however, impractical to extend the correlation time too much.

In a setup considered in this paper only range measurements are used for the localization and tracking. With other illumination signals it is sometimes desirable to include also Doppler information in the process [5], however with a Wi-Fi signal it is difficult to estimate the Doppler frequency because of the effects of non-contiguous transmission.

The conversion from the state space (described by equirange ellipses) to the measurement space of object localization is nonlinear. Typically, either the conversion is done before the tracking stage, or – as shown in this paper – an extended Kalman filter is used where the conversion is linearized at the predicted target state.

III. Wi-Fi signal properties

In recent years there has been a rapid growth of number of installed WiFi nodes. Dropping price of the equipment, ease of connection and set-up the system, and the absence of license fees for the bandwidth use enables almost anyone to build his own Wi-Fi network.

In a typical networking application, the Wi-Fi connection range varies between 75 m up to 500 m. It depends on the antenna type, antenna gain, frequency band and radio power output. With use of a directional antenna with gain of 15 dB the range may increase up to 25 km.

The OFDM modulation used in Wi-Fi standards version *g* and *n* has very good correlation properties. Together with the ubiquity of transmitters in many areas of interest, it makes Wi-Fi networks a very attractive source of the illumination for passive radars.

A Wi-Fi node working according to 802.11g standard transmits its data in short packets using a single physical channel. The arbitration of channel access is done with the CSMA/CA (Carrier-Sense Multiple Access/Collision Avoidance) method. A node ready to transmit a frame listens whether a medium is occupied or not. If it is free, it waits some time (called Distributed Coordination Function Interframe Space - DIFS) and determines randomly the time to start transmission - 'backoff'. Allocation of the channel is done using a scheme RTS - CTS (Request To Send - Clear To Send). The node wanting to start transmission sends the request packet to reserve a channel. Inside of this message the recipient identifier is placed. If the recipient does not receive any other requests at the same time, it permits for the transmission by sending a CTS packet. Other nodes in the system become silent.

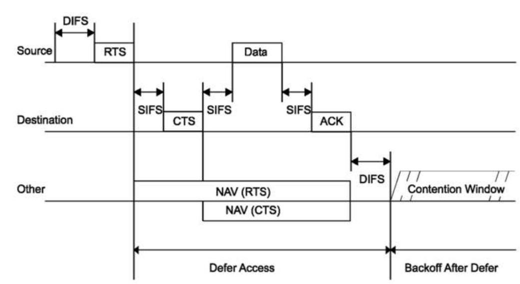

Fig. 2. CSMA/CA mechanism [13]

When the transmitting node receives the CTS packet, it sends the actual data packet to its recipient. If the RTS is not answered within predefined time, the procedure is started over again. Every time when a channel is busy the transmitting node doubles the contention window (the range of values from which a random backoff time is chosen) and generates a new random backoff period to wait before the next attempt. When the transmission of data packet is complete, the receiving station transmits an acknowledgment packet (ACK) before any other node begins to transmit a new data packet.

As it is described above, the transmission of the packets is a pulsed type with varying and unpredictable pulse durations depending on the PLCP protocol data unit (PPDU) format and on the data frame size. The PPDU frame consists of three main parts: Physical Layer Convergence Procedure Preamble (PLCP), signal and data. The training sequence, which is present in PLCP field, is used for the synchronization with the receiver.

If several nodes work in a network, one physical channel is shared between them based on time multiplexing. In order to resolve target location properly we have to know which node transmitted the signal which resulted in a measured echo. Hopefully, we can do it by decoding the data present in the "address" field of the MAC layer. According to 802.11 standard every equipment used in WiFi network has its own unique 48-bit address. The address of the transmitter and of the destination receiver are filled in the MAC header of each transmitted packet. Thus, in a WiFiRAD we need to detect the individual packages, demodulate and decode them to obtain the transmitter identifier.

Multiplexing a single channel in time with CSMA/CA method causes the majority of transmitters to be idle for significant intervals. With low traffic they are off because of the lack of data. When the traffic increases the bandwidth is wasted due to backoffs and collisions. This makes the Wi-Fi based radar suffer from low duty cycle of each transmitter.

An example of a time interval with long sequences of active transmission is shown in Fig. 3. However, more typical situation is that of Fig. 4 – with such a signal the correlation processor is fed with more gap than active signal time.

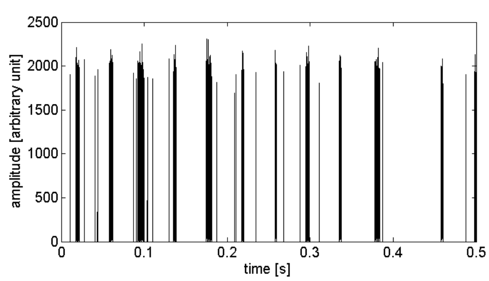

Fig. 3. An example of a high duty cycle Wi-Fi signal

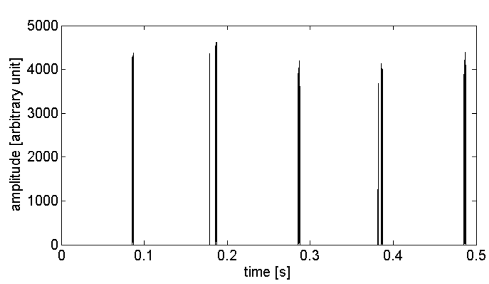

Fig. 4. An example of a low duty cycle Wi-Fi signal

Even with a high duty cycle signal the sequence of transmissions from one station is typically not longer than several tens of milliseconds.

IV. The sequential update Kalman filter

The measurements made in a radar system are combined to provide a possibly accurate location (and trajectory) of a target. In a multistatic system there are many methods for combining the measurements from different transmitter-receiver pairs.

If the measurements can be taken in the same instant, they may be either combined into an unambiguous location of the target (e.g. in Cartesian coordinates) which is then used to update the target state, or they may be used directly to do the update. In both cases all the measurements update the state in parallel – in the same instant.

In the WiFiRAD application the process of "taking" a measurement consist in correlating the reference signal with the target echo. However, if the timing of this process is chosen arbitrarily, it may happen that a particular transmitter is not active in the investigated interval – the transmitter activities are ruled by multiple access arbitration; which is totally unpredictable for the radar receiver. With an increase of the correlation time the chances of seeing the activity of all transmitter rise, but the measurements obtained are not well aligned in time, which makes the problem much more complex.

Thus, the above scheme with parallel update is hard to apply in a Wi-Fi based radar: the number of raw (bistatic) measurements available in each instant changes, and it frequently happens that the number of measurements is not enough to determine the location of the target unambiguously.

The idea of the sequential update Kalman filter application to a multistatic passive radar has been extensively described in [14]. Its advantage is the easy solution of the missing measurements problem – the tracker state is updated with each measurement separately [15]. With sequential update scheme the tracker state is updated at the moment when a measurement is available. This allows to perform the update without waiting for all the measurements; also, the alignment of the measurements in time is not necessary.

In a sequential update scheme used in this paper, the state vector of the target is written at k-th observation in 2D Cartesian coordinates as usual [14]:

$$\boldsymbol{x}(k) = [x(k), v_x(k), y(k), v_y(k)]^T \tag{3}$$

The state vector evolution consists of a predicted state and noise contribution:

$$\boldsymbol{x}(k) = \mathbf{F}\boldsymbol{x}(k-1) + \boldsymbol{w}(k) \tag{4}$$

where F is:

$$\mathbf{F} = \begin{bmatrix} 1 & T & 0 & 0 \\ 0 & 1 & 0 & 0 \\ 0 & 0 & 1 & T \\ 0 & 0 & 0 & 1 \end{bmatrix} \tag{5}$$

and T is time step between observations. The time step is actually variable, as the measurements are not uniformly spaced in time, but we omit it for the simplicity of notation. The process noise vector $\boldsymbol{w}(k)$ has covariance $\mathbf{Q}$:

$$\mathbf{Q} = \begin{bmatrix} \mathbf{G}\sigma_{wx}^2 & \mathbf{0} \\ \mathbf{0} & \mathbf{G}\sigma_{wy}^2 \end{bmatrix} \tag{6}$$

where σ_{wx}^2 and σ_{wy}^2 are the variances of the x and y components of the process noise, and $\mathbf{G}$ is:

$$\mathbf{G} = \begin{bmatrix} \frac{T^2}{2} & T \\ T & 1 \end{bmatrix} \tag{7}$$

The noisy observation vector corresponding to m-th transmitter is actually a scalar since it consists of the bistatic range measurement only (in the presented approach we do not use the Doppler velocity). It is modeled with the following equation (please note that ^{m} is an index, not a power here):

$$\boldsymbol{z}^m(k) = \boldsymbol{h}^m(\boldsymbol{x}(k-1)) + \boldsymbol{v}^m(k) \tag{8}$$

where $\boldsymbol{v}^m$ covariance is known as $\mathbf{R}^m = \sigma_{R_b}^2$ and m is a measurement index.

As the function h^m is nonlinear, we use the Extended Kalman Filter (EKF) approach and linearize it at predicted state $\hat{\boldsymbol{x}}(k|k-1)$, obtaining a vector $\mathbf{H^m(k)}$of derivatives w.r.t. the elements of the state vector.

The Kalman filter step consists of the prediction of the state vector and its covariance matrix:

$$\hat{\boldsymbol{x}}(k|k-1) = \mathbf{F}\hat{\boldsymbol{x}}(k-1|k-1) \tag{9}$$

$$\mathbf{P}(k|k-1) = \mathbf{F}\mathbf{P}(k-1|k-1)\mathbf{F}^T + \mathbf{Q} \tag{10}$$

and the sequence of updates with M available measurements $m = 1, 2...M$, iterating over m. The starting values for the update $\hat{\boldsymbol{x}}(k|k-1)^0 = \hat{\boldsymbol{x}}(k|k-1)$ and $\mathbf{P}(k|k-1)^0 = \mathbf{P}(k|k-1)$ are taken from the prediction stage. Then, the following is repeated M times:

$$\mathbf{S}^m(k) = \mathbf{H}^m(k)\mathbf{P}^{m-1}(k|k-1)(\mathbf{H}^m(k))^T + \mathbf{R}^m \tag{11}$$

$$\mathbf{K}^m(k) = \mathbf{P}^{m-1}(k|k-1)(\mathbf{H}^m(k))^T(\mathbf{S}^m(k))^{-1} \tag{12}$$

$$\boldsymbol{v}^m(k) = \boldsymbol{z}^m(k) - \boldsymbol{h}^m\big(\hat{\boldsymbol{x}}(k|k-1)\big) \tag{13}$$

$$\hat{\boldsymbol{x}}^m(k|k-1) = \hat{\boldsymbol{x}}^{m-1}(k|k-1) + \mathbf{K}^m(k)\boldsymbol{v}^m(k) \tag{14}$$

$$\mathbf{P}^m(k|k-1) = \big(\mathbf{I} - \mathbf{K}^m(k)\mathbf{H}^m(k)\big)\mathbf{P}^{m-1}(k|k-1) \tag{15}$$

The final values of $\hat{\boldsymbol{x}}$ and $\mathbf{P}$ (with index ^{M}) are used as the result of the whole update sequence, $\hat{\boldsymbol{x}}(k|k)$ and $\mathbf{P}(k|k)$.

V. Experiment description

The experiment was performed in August 2014 on a greenfield near Mierzanowo village in central Poland. The location was free from external Wi-Fi signals. Position of the Wi-Fi nodes has been presented on the Fig. 5. Distance between radar and Wi-Fi network nodes was between 150 to 200m.

As a target for the radar system a small car presented in Fig. 6 was used. The target was moving with approximately constant speed. The analysis of the WiFiRAD ability to detect the targets with similar RCSs had been performed and confirmed experimentally in previous papers [8], [16]. Main difference from previous experiments was the higher number of illuminators and smaller area. Such setup was chosen in order to test developed target tracking algorithms on the experimental data.

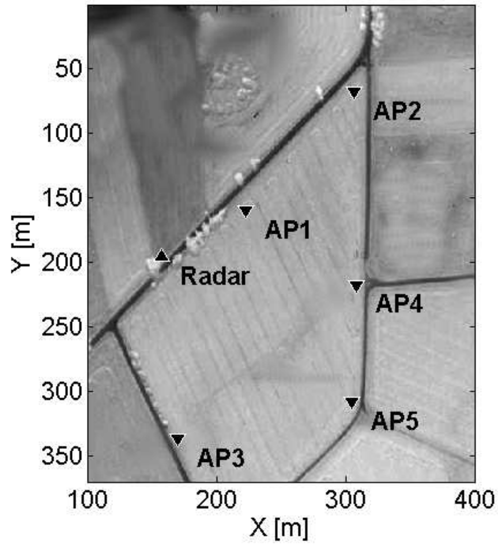

Fig. 5. System layout

The Wi-Fi network built for the experiment had 5 nodes, served by MikroTik Routerboards RB433Ah and RB600 with extended sensitivity cards (RouterBoard-R52Hn). All nodes used omnidirectional 17 dBi antennas.

The data traffic was mainly UDP generated by MikroTik bandwidth test application. A small amount of ICMP traffic (ping) between Wi-Fi network nodes has been added to increase reality of the experiment.

The passive radar consisted of

- an omnidirectional antenna with high vertical plane gain which gathered reference signals from all the nodes,
- a highly directional antenna (14° horizontal and 10° vertical) which was pointed to the area of interest
- a two-channel vector signal analyzer recording signal with 36 MHz bandwidth.

Both antennas are shown in Fig. 7.

Fig. 6. The target

Fig. 7. System antennas

VI. Signal processing

Signals collected during the campaign where processed in off-line mode using Matlab environment. Fig. 8 shows a general processing scheme. As it was mentioned before, the first step in such system is to determine the source of transmission and separate signals coming from different access points. The transmitter address of each recorded frame is extracted during the demodulation and decoding process. At this point it is worth to mention that a Wi-Fi signal sampled without hardware synchronization requires special demodulation and digital synchronization process which, in general, is very similar to one described in [17].

The reference signal is reconstructed according to the standard specification to obtain clear, not channel-disturbed transmitted signal. The echo signal is processed with an adaptive filter to get rid of the stationary echoes (clutter). At this stage the reference and echo waveforms are divided in

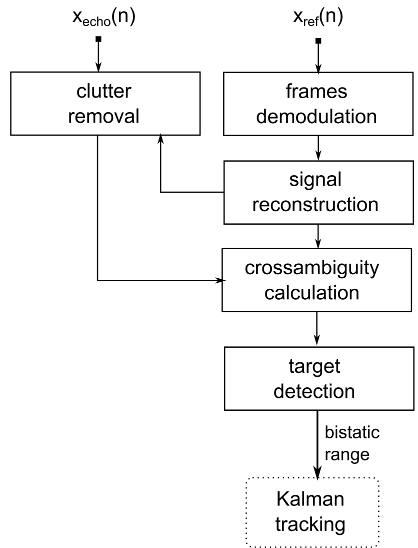

Fig. 8. Processing scheme

short (100 ms length) blocks, in order to avoid too many gaps in the transmission. The blocks with enough active transmit time enter the correlation receive where the cross ambiguity function is calculated. Maxima of this function determine the bistatic range for each transmitter-receiver pair at each time interval. These range values are finally input to a sequential Kalman filter.

The Kalman filter initial state was determined using classical method in the first moment when data was sufficient (number of measurements per interval was equal or greater than three).

VII. Results

As expected, the recordings show that the number of active nodes in different time intervals varies randomly. Fig. 9 shows available measurements in terms of time for one of the recordings. It is clearly visible that in many periods the data is insufficient to perform a classical ellipse-intersection localization. There are also moments where completely no measurement is available.

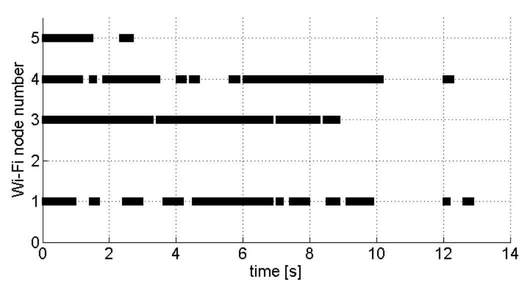

Fig. 9. Measurements availability

The tracking was quite correct, especially regarding the varying availability of transmitter illuminations. Fig. 10 shows measurement scenario (node localizations and actual target path) and results of tracking. The target (a car) was moving along the road marked with a wide black line.

The localization error as a function of time is shown in Fig. 11 together with the number of transmitters whose measurements were available in each 100 ms interval. It should be noted that for the majority of time this number was insufficient for a 2D localization with ellipse crossing method.

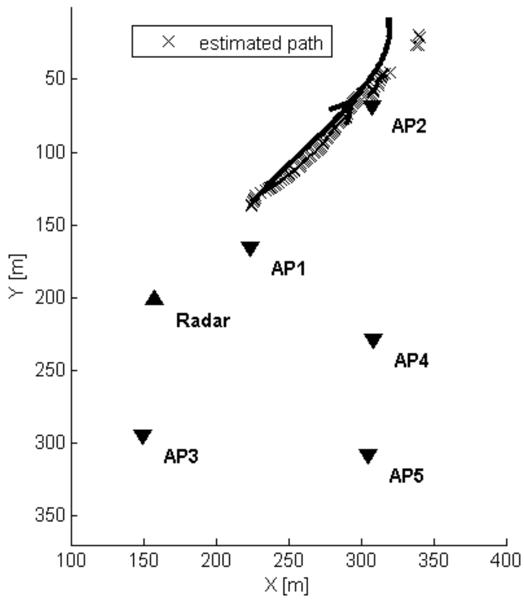

Fig. 10. Estimated and actual target path

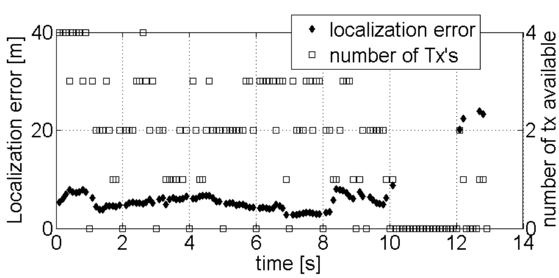

Fig. 11. Tracking error in terms of time

One can notice that periods with lower error level correlate mostly with three or four available measurements. However, with less measurements the error does not increase significantly. The exception can be seen at the end of the experiment, where, after a long no-detection period, the Kalman filter is fed only with single-source bistatic measurements. This is the main reason why the tracker was unable to detect the car turning.

The weak point of the algorithm is the state initialization. It is obvious that the set of measurements used for initialization must allow unambiguous localization of the target. In consequence, a track cannot be initialized in arbitrary instant. Even with enough measurements the initial state is estimated with some error.

The error of the first localization propagates throughout whole tracking process. Fig. 12 and Fig. 13 show the tracker accuracy for several arbitrarily chosen start points scattered around the real start. One can see that in this case the initial error causes continuous path wandering around the correct path. It should be, however, noticed that despite the initial error the track goes in correct direction from a relatively wide starting area. These effects depend on system geometry, current object localization and Kalman filter parameters. An interesting investigation into this subject can be found in [10].

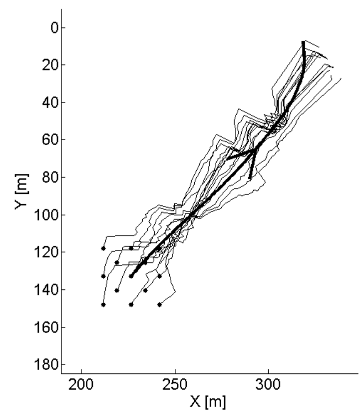

Fig. 12. Start point sensitivity

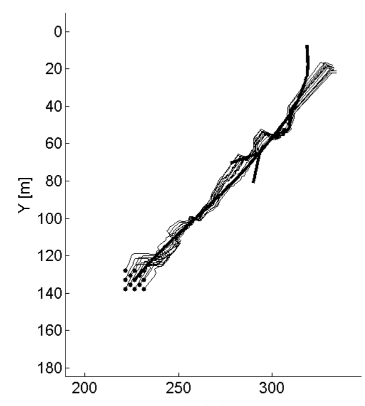

Fig. 13. Start point sensitivity

Fig. 14 shows a comparison between proposed sequential and parallel updated tracking algorithm. First of all, it must be noted that in order to perform parallel update the signal integration time had to be extended so that enough measurements were collected. When sequential update was applied with 100 ms integration time, the parallel update required at least 500 ms. In Fig. 14 results of parallel update tracking for integration times of half and one second are shown. It can be noticed that full measurement sets occurred only in first few seconds, therefore the tracking path ends faster then in sequential update. Secondly, larger errors may occur because the update is performed at the end of the integration interval, but particular measurements actually pertain to a small fraction of the interval when the relevant transmitter was active. This may cause significant errors especially when transmitters are active in bursts.

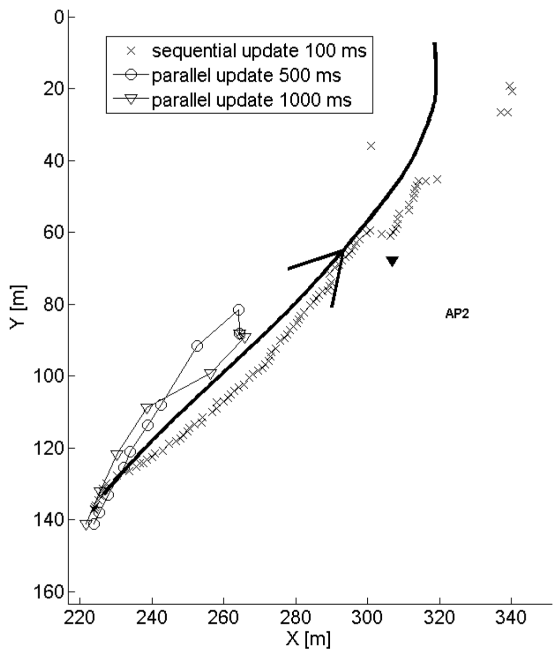

Fig. 14. Algorithms comparison

VIII. Conclusion

A full scheme of Wi-Fi radar signal processing from the antenna to the tracker has been presented in the paper. Specific difficulties arising from the random transmission activity due to access arbitration have been addressed.

The results of processing the experimental data confirm the usability of the proposed concept. The processing and tracking scheme allows the utilization of all the measurements, even if their set available at the particular instant is too small for unambiguous localization.

Short range of a system, its modest accuracy and very specific requirements for successful operation (such as high number of WiFi nodes) limit its potential applications. It is possible to use such a system in areas like airports, shopping malls, parking yards or warehouses, as a smart surveillance or alarm system. Other application can be traffic intensity measurements or a collision detection system.

With advanced clutter removal and more sophisticated signal correlation, which is planned as a future work, it will be possible to take advantage of Doppler measurements as well. This improvement will definitely result in higher tracking precision.

References

[1] K. S. Kulpa, "Multi-static entirely passive detection of moving targets and its limitations," *IEE Proceedings Radar, sonar and navigation*, vol. 152, no. 3, pp. 169–173, June 2005.

[2] H. Griffiths and C. Baker, "Passive coherent location radar systems. Part 1: performance prediction," *Radar, Sonar and Navigation, IEE Proceedings* -, vol. 152, no. 3, pp. 153 – 159, Jun. 2005.

[3] K. Kulpa, M. P. Malanowski, P. J. Samczyński, P. Krysik, and S. Rzewuski, "Application of communication signals for remote sensing," in *Proceedings of the Conference on Electronics Telecommunications and Computers*, 2013, pp. 1–6.

[4] K. Kulpa, M. P. Malanowski, P. J. Samczyński, P. Krysik, S. Rzewuski, and E. Śliwa, "Application of communication signals for remote sensing," *Procedia Technology*, vol. 17, 2014.

[5] P. Krysik, M. Wielgo, J. Misiurewicz, and A. Kurowska, "Doppler-only tracking in GSM-based passive radar," in *International Conference on Information Fusion 2014*, 2014.

[6] S. Rzewuski and K. Kulpa, "System concept of WiFi based passive radar," *International Journal of Electronics and Telecommunications*, vol. 57, no. 4, 2011.

[7] K. Kulpa, S. Rzewuski, Z. Gajo, and M. P. Malanowski, "Concept of multistatic passive radar based on wireless packet communication systems," in *Proceedings of 2011 IEEE CIE International Conference on Radar*, S. Wu, Ed., 2011.

[8] S. Rzewuski, M. Wielgo, K. Kulpa, M. P. Malanowski, and J. Kulpa, "Multistatic passive radar based on WiFi – results of the experiment," in *2013 International Conference on Radar*, Adelaide, Australia, 2013.

[9] F. Colone, P. Falcone, C. Bongioanni, and P. Lombardo, "WiFi-based passive bistatic radar: Data processing schemes and experimental results," *Aerospace and Electronic Systems, IEEE Transactions on*, vol. 48, no. 2, pp. 1061–1079, Apr. 2012.

[10] I. Ivashko, O. Krasnov, and A. Yarovoy, "Receivers topology optimization of the combined active and wifi-based passive radar network," in *European Radar Conference (EuRAD), 2014 11th*, Oct 2014, pp. 517–520.

[11] P. Falcone, F. Colone, A. Macera, and P. Lombardo, "Two-dimensional location of moving targets within local areas using WiFi-based multistatic passive radar," *Radar, Sonar Navigation, IET*, vol. 8, no. 2, pp. 123–131, February 2014.

[12] B. Manavoglu and E. Yazgan, "Tracking of real airborne targets with multistatic passive radars in 3D," in *Radar Symposium (IRS), 2014 15th International*, June 2014, pp. 1–6.

[13] IEEE Standard for Information technology – Telecommunications and information exchange between systems – Local and metropolitan area networks – Specific requirements Part 11: Wireless LAN Medium Access Control (MAC) and Physical Layer (PHY) Specifications.

[14] M. Malanowski, K. Kulpa, and R. Suchożebrski, "Two-stage tracking algorithm for passive radar," in *Information Fusion, 2009. FUSION '09. 12th International Conference on*, July 2009, pp. 1800–1806.

[15] Y. Bar-Shalom and X.-R. Li, *Multitarget-multisensor tracking: Principles and techniques*. Storrs (US): Yaakov Bar-Shalom, 1995, index.

[16] S. Rzewuski, M. Wielgo, K. Klincewicz, Ł. Podkalicki, K. Kulpa, and M. P. Malanowski, "Multistatic wireless fidelity network based radar: Results of the Chrcynno experiment," *Radioengineering*, vol. 23, 2014.

[17] M. Baczyk and M. Malanowski, "Decoding and reconstruction of reference DVB-T signal in passive radar systems," in *Radar Symposium (IRS), 2010 11th International*, June 2010, pp. 1–4.